Pinning and Avalanches in Hydrophobic Microchannels

M. Queralt-Martín,[1] M. Pradas,[1,2] R. Rodríguez-Trujillo,[3] M. Arundell,[3]
E. Corvera Poiré,[4,*] and A. Hernández-Machado[1,†]

[1]*Departament ECM, Facultat de Física, Universitat de Barcelona, Diagonal 647, E-08028 Barcelona, Spain*
[2]*Department of Chemical Engineering, Imperial College London, London, SW7 2AZ, United Kingdom*
[3]*Departament Electrónica, Facultat de Física, Universitat de Barcelona, Diagonal 647, E-08028 Barcelona, Spain*
[4]*Departamento de Física y Química Teórica, Facultad de Química, Universidad Nacional Autónoma de México,
México DF 04510, Mexico*
(Received 21 September 2010; published 10 May 2011)

Rare events appear in a wide variety of phenomena such as rainfall, floods, earthquakes, and risk. We demonstrate that the stochastic behavior induced by the natural roughening present in standard microchannels is so important that the dynamics for the advancement of a water front displacing air has plenty of rare events. We observe that for low pressure differences the hydrophobic interactions of the water front with the walls of the microchannel put the front close to the pinning point. This causes a burstlike dynamics, characterized by series of pinning and avalanches, that leads to an extreme-value Gumbel distribution for the velocity fluctuations and a nonclassical time exponent for the advancement of the mean front position as low as 0.38.

PACS numbers: 47.61.−k, 47.55.dr, 47.55.np

Controlling the advancement of a fluid inside a microchannel is one of the main issues in microfluidics. The huge amount of technological, biological, and medical applications found in the miniaturization of fluidic systems has required considerable effort in order to understand the physics of microfluidics [1–6]. As downsizing leads to an increased surface-to-volume ratio, surface properties of the microchannel, such as wetting and roughness, are of fundamental importance since they would largely determine the large or low resistance to flow [4,7–12]. They will also determine, together with the driving pressure, the total or partial impregnation of the microchannel. For instance, for hydrophobic interactions and low pressures, a state can be reached in which the fluid does not totally impregnate the microchannel. This is known as the fakir state and has been observed in nanopatterned surfaces [4,7]. A different way of characterizing surface properties is to understand the underlying mechanisms in the dynamics of the advancement of a water front. For example, while a hydrophobic microchannel is being filled, one might conceive situations in which the water front experiences either low resistance to flow or high resistance to flow (as shown in the present work) depending on the type of disorder encountered by the front.

We study the dynamics of a water front displacing air at constant pressure difference into a polydimethylsiloxane (PDMS) hydrophobic microchannel with the natural roughening present during its fabrication using a standard soft-lithography protocol [13–15], i.e., without a deliberate controlled nanopattern engraved. Our experimental results show that the advancement of the front at low pressure differences is characterized by a series of pinning and avalanches that leads to a dynamics of rare events.

Extreme-value distributions deal with the stochastic behavior of the extremes of independent and identically distributed random variables. The most common of these types of distributions is the Gumbel distribution [15–18]. It has been found to describe physical phenomena in fracture cracks, granular materials, fluctuations near a critical point, and imbibition of fluids in porous media [19–25]. We find that the velocity fluctuations during the advancement of the water front in a hydrophobic microchannel follow a BHP-Gumbel distribution [26] that characterizes the rare events observed.

The experimental setup is illustrated in Fig. 1 (see [15] for details). We track the interface position as a function of time and find that the mean front advances with a power law in time $h \sim t^\nu$. Figure 2(a) shows $h(t)$ for two different applied pressure differences. At low driving pressure differences, we obtain a nonclassical exponent of value as low as $\nu = 0.38$. Detailed analysis of the data reveals a dynamics of pinning and avalanches. More precisely,
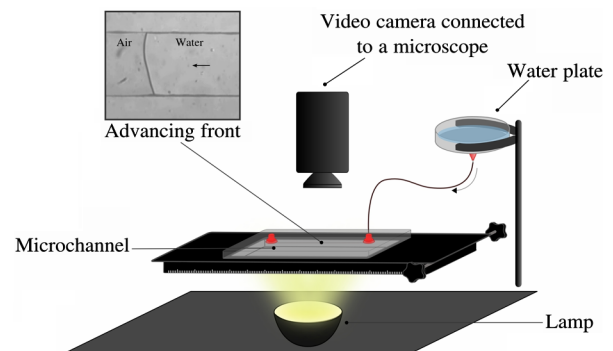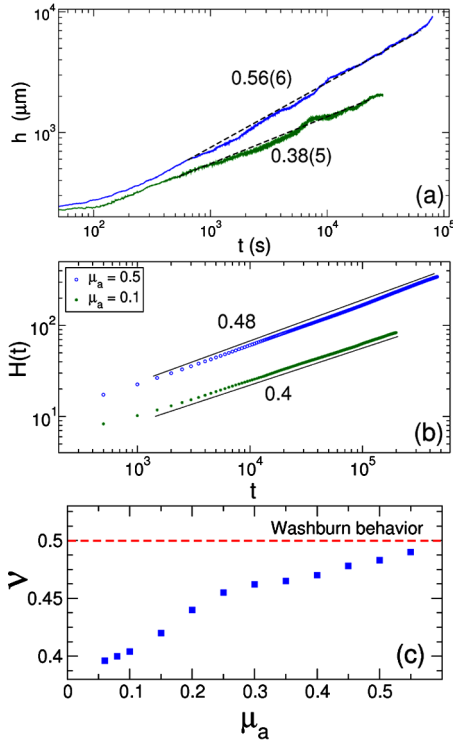

FIG. 1 (color online).   Experimental setup.

FIG. 2 (color online). (a) Experimental results of the mean front position $h(t) \sim t^{\nu}$ in a hydrophobic microchannel for two different pressure differences. (b) Numerical results for $h(t)$ in a hydrophobic microchannel for two different pressure differences. (c) Asymptotic value of the exponent as a function of the applied pressure difference.
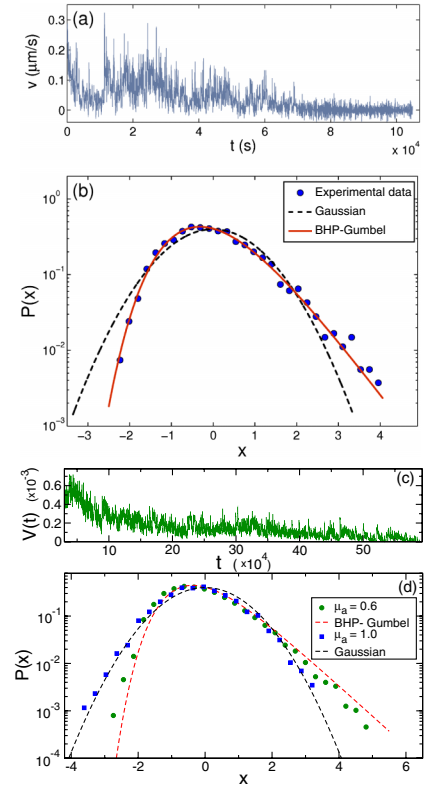

FIG. 3 (color online). (a) Experimental evolution of the front velocity $v(t)$ (μm/s) at small pressure difference. (b) Distribution of experimental velocity fluctuations in the variable x (see text) fitted to both a BHP-Gumbel and a Gaussian distribution. (c) Numerical evolution of the front velocity $v(t)$. (d) Distribution of numerical velocity fluctuations fitted to both a BHP-Gumbel and a Gaussian distribution.

we observe small time intervals for which the slope of the front position versus time is close to zero (pinning points), which are followed by sudden advances of the interface (avalanches). In other words, for small pressure differences, the advancement of the front is affected by local pinning-depinning of the contact line between the fluid and the rough surface. This induces cooperative correlated motion, which is reflected as a burstlike dynamics of the front. For higher pressure differences, the system is far from the pinning point, and the advancement of the front is consistent with the classical Washburn dynamics, for which at a constant pressure difference the front advances with an exponent $\nu \gtrsim 1/2$ and goes asymptotically to $\nu = 1/2$ as $t \to \infty$.

We compute the velocity of the front $v(t)$ by taking the time derivative of $h(t)$. Figure 3(a) shows the velocity for the front whose advancement at low pressures is shown in Fig. 2(a). Typical velocities during avalanches are of the order of 0.3 μm/s which, for water advancing through the microchannel used in these experiments, gives Reynolds numbers of the order of Re $\sim 10^{-5}$. Since the front proceeds by imposing a constant pressure difference, the mean velocity decays with time. We have subtracted the mean value of the velocity in order to study velocity fluctuations $\delta v(t)$ around the mean. We consider the probability distribution of the variable $x = \frac{\delta v}{\sigma_v}$, where σ_v is the vari-

ance. We find that the distribution of the velocity fluctuations is given by a BHP-Gumbel distribution, which is characterized for having a long tail at large velocity fluctuations. This is illustrated in Fig. 3(b), where a comparison to a Gaussian distribution is also presented. We have also analyzed the velocity fluctuations distribution at large driving pressure differences and obtained a Gaussian distribution (not shown). This is because in this situation the pinning effects are overcome by the driving force.

In order to consider wetting effects we introduce a phase field model in three dimensions that allows for hydrophilic and hydrophobic interactions with the walls. Surface roughening is modeled by considering obstacles of arbitrary shapes randomly distributed along the microchannel walls. In this model, a field ϕ is used to represent the two existing phases, whose equilibrium properties are given by a Ginzburg-Landau model with a free energy of the form

$$\mathcal{F}[\phi] = \int d\mathbf{r}[(\epsilon \boldsymbol{\nabla} \phi)^2/2 - \phi^2/2 + \phi^4/4] - \int_s ds f_s(\phi_s),$$

(1)

where f_s takes into account the fluid interactions with the wall [27], and it is taken as $f_s = A_s \phi_s$, where ϕ_s is the

value of the phase field at the wall, and A_s is a parameter that describes the preference of the wall for either the liquid phase ($A_s > 0$, for hydrophilic interactions) or the air phase ($A_s < 0$, for hydrophobic interactions). The locally conserved dynamics is then described by

$$\partial_t \phi = \nabla \cdot M \nabla \mu = \nabla \cdot M \nabla [-\phi + \phi^3 - \epsilon^2 \nabla^2 \phi], \quad (2)$$

with the natural boundary condition at the walls,

$$\left. \frac{df_s}{d\phi} \right|_s = \epsilon^2 [\hat{\mathbf{n}} \cdot \nabla \phi]_s, \quad (3)$$

where M is a mobility parameter which we take constant in the liquid phase ($\phi > 0$) and zero in the air phase ($\phi < 0$), and μ is the chemical potential. The wetting boundary condition, Eq. (3), should be applied with the proper value of the parameter A_s all along the walls, both for rough and smooth boundaries. To study the time evolution of a front, the applied pressure at the inlet of the microchannel is fixed through a constant value for μ.

In order to understand the effect of the pinning-depinning of the contact line between the front and the obstacles forming the roughness of the microchannel wall, we first model the advancement of a front penetrating a rectangular microchannel where the roughening consists of obstacles in the shape of steps perpendicular to the flow direction, randomly distributed along the flow direction, and infinitely large in the direction transverse to the flow [Fig. 4(a)]. We consider steps of fixed height h_d and arbitrary lengths l_d which are separated by arbitrary distances l_g. We integrate Eq. (2) subject to the boundary condition, Eq. (3), with $A_s < 0$ all along the hydrophobic microchannel walls [15]. Figure 4(a) shows how air phase regions are being trapped between the steps of the rough wall as the water front moves forward. This illustrates that our model accounts correctly for the fakir state. Figure 4(b) (left) shows a detail of such a fakir state in which the fluid does not totally impregnate the microchannel.
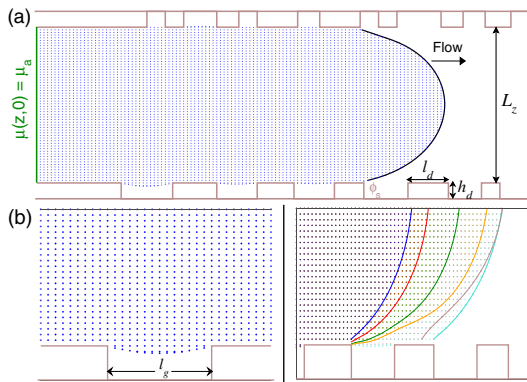

FIG. 4 (color online). (a) Microchannel with roughness in the form of steps and the water front that has left an air phase trapped between the structures that form the roughness. (b) (left) Detail of the fakir state, (right) detail of the contact line at different times.

Depending on the applied pressure difference, the fluid would impregnate the substrate in different degrees. Finally, Fig. 4(b) (right) shows a detail of the advancement of the contact line at low applied pressure difference, at different times. It is possible to see how the contact line gets pinned at a step edge and suddenly jumps towards the next step along the flow. For very high applied pressures, the fluid totally impregnates the channel and the fakir state is no longer observed.

Figure 2(b) shows the mean advancement of the front $h(t) \sim t^\nu$ for two typical applied pressures. The exponent ν has the value 0.4 for a typical low applied pressure difference and the value $\nu = 0.48$ for a typical high applied pressure difference, which are in good agreement with experiments. Figure 2(c) shows the asymptotic value of the exponent for different applied pressures. As the driving force increases, the asymptotic value of the exponent grows relatively fast up to values of around 0.46. After that, it has a crossover behavior in the slope and continues increasing until it reaches the Washburn exponent 0.5. For the asymptotic behavior the exponent value is never larger than 0.5. We have observed the same qualitative behavior for different distributions of the obstacles forming the rough walls. Our results indicate that the crossover pressure depends upon the statistical properties of the microchannel. An exponent smaller than 0.5 is only observed at sufficiently low values of the applied pressure for which the interface is characterized by strong pinning effects.

To rationalize a nonclassical exponent at low pressures, we propose a description, based on an effective Darcy's law in which the roughness of the channel induces an effective mean curvature that depends on time $\bar{\kappa}(t)$:

$$\frac{dh(t)}{dt} = K \left[\frac{p_a - \sigma \bar{\kappa}(t)}{h(t)} \right], \quad (4)$$

where $K = b^2/12\eta$ is the permeability, which is related to the mobility parameter of the phase field as $K = M/2$, b is the microchannel thickness, η is the dynamic viscosity, p_a is the applied pressure at the origin, and $\sigma \bar{\kappa}$ is the pressure drop across the interface. Without loss of generality we take the pressure in the air equal to zero. Note that Eq. (4) can also be written as

$$\frac{dh^2(t)}{dt} = M [p_a - \sigma \bar{\kappa}(t)]. \quad (5)$$

The actual time dependence of the curvature is something that is not known *a priori* and must contain the main physical mechanism that causes the pinning-depinning dynamics of the contact line. Figure 5 shows that the numerical integration of our model is in very good agreement with Eqs. (4) and (5). Moreover, using the exponent value obtained for $h(t)$ at this typical low pressure, $\nu = 0.4$, we see that the relations $\frac{dh(t)}{dt} \sim t^{-0.6}$ and $\frac{dh^2(t)}{dt} \sim t^{-0.2}$ must hold. This is confirmed by the overall behavior of the curves presented in Fig. 5. These results show that a description based on an effective Darcy's law,
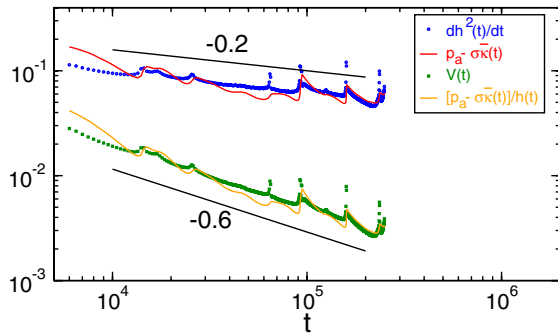
FIG. 5 (color online). Numerical results independently computed for the left- and right-hand sides of Eqs. (4) and (5). Agreement with an effective Darcy's law is found.

with an effective time-dependent curvature determined by the pinning-depinning of the contact line, is consistent with a nonclassical exponent for the front advancement.

In order to study avalanche dynamics, we consider that obstacles randomly distributed on the upper and lower walls of the rectangular microchannel with the same value of A_s [see text after Eq. (1)] can be mapped into a two-dimensional system with patches of two different degrees of effective hydrophobicity. Note that the different degree of hydrophobicity of the patches is due to the presence of the rough structure. Such a projected description is correctly described by a dichotomic quenched disorder field, $\eta(\mathbf{r}) < 0$. In this case, the free energy takes the form $\mathcal{F}[\phi] = \int d\mathbf{r}[(\epsilon\boldsymbol{\nabla}\phi)^2/2 - \phi^2/2 + \phi^4/4 - \eta(\mathbf{r})\phi]$, with a dynamic equation for ϕ of the form [28]

$$\partial_t\phi = \boldsymbol{\nabla} \cdot M\boldsymbol{\nabla}[-\phi + \phi^3 - \epsilon^2\nabla^2\phi - \eta(\mathbf{r})]. \quad (6)$$

Figures 3(c) and 3(d) show the numerical results obtained by numerical integrations of Eq. (6) [15]. Comparison with the experimental results presented in Figs. 3(a) and 3(b) shows that the model correctly describes the cooperative correlated motion of the front which is reflected as a burstlike dynamics. This in turn gives rise to an extreme-value distribution for the velocity fluctuations, which is correctly characterized by a BHP-Gumbel distribution. We observe this behavior, both numerically and experimentally, whenever the exponent ν is smaller than 0.5. For relatively higher applied pressures, we observe the Washburn exponent, but we can still observe a Gumbel distribution for the velocity fluctuations. Only at very high applied pressures, when the pinning effects are completely overcome by the high velocity of the interface, we observe a Washburn exponent for the interface growth and a Gaussian distribution for the velocity fluctuations.

In conclusion, the experimental behavior observed during the filling of hydrophobic microchannels shows a burstlike dynamics, leading to nonclassical exponents for the advancement of the mean front and extreme-value distributions for the velocity fluctuations. We can interpret these results in the context of a front propagating in a rough hydrophobic microchannel. Our results are potentially

relevant in the context of lab-on-a-chip and micro-total-analysis devices. We have proved that with standard fabrication procedures a burstlike dynamics and a slow advancement of the front would be inevitably present due to the natural roughness present on the microchannel. If one wanted to suppress these effects, nanopatterning of the microchannels should be considered.

*eugenia.corvera@gmail.com
†a.hernandezmachado@gmail.com

[1] T. Squires and S. Quake, Rev. Mod. Phys. **77**, 977 (2005).
[2] P. Tabeling, *Introduction to Microfluidics* (Oxford University Press, New York, 2006).
[3] E. Lauga, M. Brenner, and H. Stone, in *Handbook of Experimental Fluid Mechanics*, edited by C. Tropea, A. Yarin, and J.F. Foss (Springer-Verlag, Berlin, 2007), p. 1219.
[4] C. Cottin-Bizonne *et al.*, Nature Mater. **2**, 237 (2003).
[5] G. Whitesides, Nature (London) **442**, 368 (2006).
[6] J.G. Santiago *et al.*, Exp. Fluids **25**, 316 (1998).
[7] M. Sbragaglia and A. Prosperetti, Phys. Fluids **19**, 043603 (2007).
[8] C. Ybert *et al.*, Phys. Fluids **19**, 123601 (2007).
[9] J. Hyvaluoma and J. Harting, Phys. Rev. Lett. **100**, 246001 (2008).
[10] P.G. de Gennes, Langmuir **18**, 3413 (2002).
[11] C. Kunert and J. Harting, Phys. Rev. Lett. **99**, 176001 (2007).
[12] H. Kusumaatmaja *et al.*, Phys. Rev. E **77**, 067301 (2008).
[13] J.C. McDonald *et al.*, Electrophoresis **21**, 27 (2000).
[14] R. Rodriguez-Trujillo *et al.*, Microfluid. Nanofluid. **3**, 171 (2006).
[15] See supplemental material at http://link.aps.org/supplemental/10.1103/PhysRevLett.106.194501 for details on methods.
[16] E.J. Gumbel, *Statistics of Extremes* (Columbia University Press, New York, 1958).
[17] S.T. Bramwell, Nature Phys. **5**, 444 (2009).
[18] E. Bertin, Phys. Rev. Lett. **95**, 170601 (2005).
[19] D. Bonamy, S. Santucci, and L. Ponson, Phys. Rev. Lett. **101**, 045501 (2008).
[20] K.J. Maloy *et al.*, Phys. Rev. Lett. **96**, 045501 (2006).
[21] A. Daerr and S. Douady, Nature (London) **399**, 241 (1999).
[22] S. Joubaud *et al.*, Phys. Rev. Lett. **100**, 180601 (2008).
[23] M. Rost *et al.*, Phys. Rev. Lett. **98**, 054502 (2007).
[24] R. Planet, S. Santucci, and J. Ortin, Phys. Rev. Lett. **102**, 094502 (2009).
[25] M. Pradas, J.M. Lopez, and A. Hernandez-Machado, Phys. Rev. E **80**, 050101(R) (2009).
[26] S.T. Bramwell, P.C.W. Holdsworth, and J.-F. Pinton, Nature (London) **396**, 552 (1998).
[27] J.W. Cahn, J. Chem. Phys. **66**, 3667 (1977).
[28] M. Pradas, Ph.D. thesis, University of Barcelona, 2009.